AD-A044 545 NAVAL SURFACE WEAPONS CENTER WHITE OAK LAB SILVER SP--ETC F/G 20/2
THE CRYSTAL STRUCTURE STUDY OF LI5B4.(U)
JUN 77 F E WANG, M A MITCHELL, R A SUTULA

UNCLASSIFIED NSWC/WOL/TR-77-84 NL

1 OF 1
ADA044545

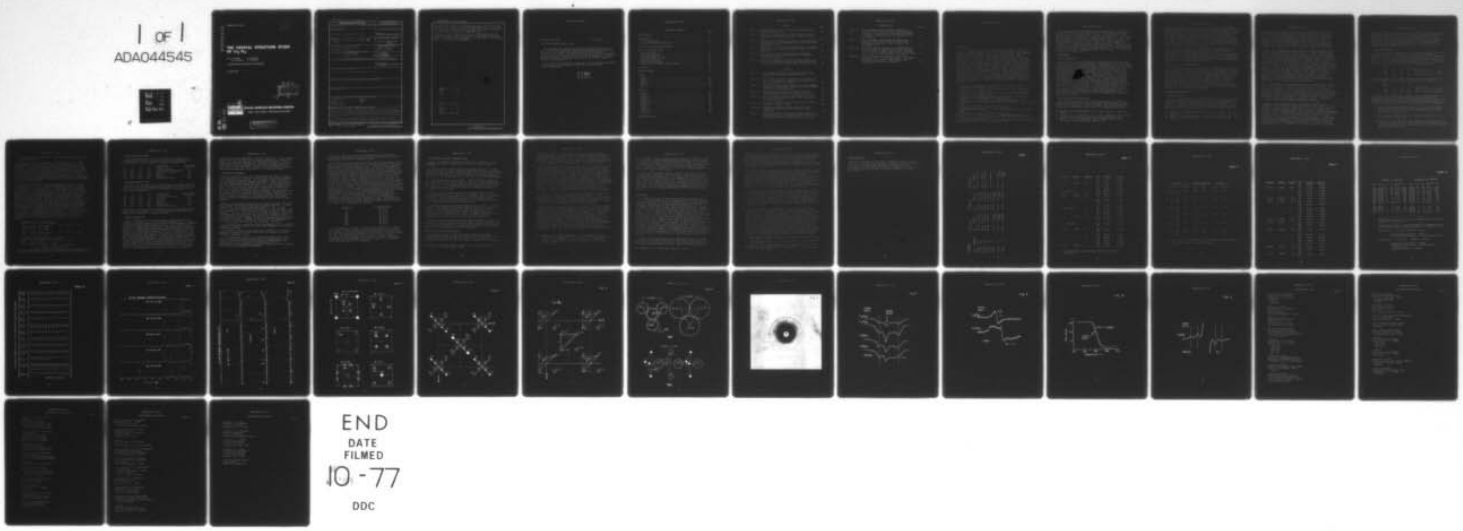

END
DATE FILMED
10-77
DDC

NSWC/WOL TR 77-84

12

THE CRYSTAL STRUCTURE STUDY OF Li_5B_4

BY F. E. WANG R. A. SUTULA
M. A. MITCHELL J. R. HOLDEN

RESEARCH AND TECHNOLOGY DEPARTMENT

22 JUNE 1977

NAVAL SURFACE WEAPONS CENTER

Dahlgren, Virginia 22448 • Silver Spring, Maryland 20910

UNCLASSIFIED

SECURITY CLASSIFICATION OF THIS PAGE (When Data Entered)

REPORT DOCUMENTATION PAGE

READ INSTRUCTIONS BEFORE COMPLETING FORM

1. REPORT NUMBER: NSWC/WOL/TR-77-84	2. GOVT ACCESSION NO.
3. RECIPIENT'S CATALOG NUMBER	
4. TITLE (and Subtitle): The Crystal Structure Study of Li_5B_4	5. TYPE OF REPORT & PERIOD COVERED: Final TR
6. PERFORMING ORG. REPORT NUMBER	
7. AUTHOR(s): F. E. Wang, M. A. Mitchell, R. A. Sutula, and J. R. Holden	8. CONTRACT OR GRANT NUMBER(s): ONR Contract N00014-7TWR-T0030-
9. PERFORMING ORGANIZATION NAME AND ADDRESS: Naval Surface Weapons Center, White Oak Laboratory, White Oak, Silver Spring, Maryland 20910	10. PROGRAM ELEMENT, PROJECT, TASK AREA & WORK UNIT NUMBERS: 61153N; PR01302; RR0130243; WR32AA;
11. CONTROLLING OFFICE NAME AND ADDRESS	12. REPORT DATE: 22 June 1977
	13. NUMBER OF PAGES: 40
14. MONITORING AGENCY NAME & ADDRESS (if different from Controlling Office)	15. SECURITY CLASS. (of this report): UNCLASSIFIED
	15a. DECLASSIFICATION/DOWNGRADING SCHEDULE

16. DISTRIBUTION STATEMENT (of this Report)

Approved for Public Release; Distribution Unlimited

17. DISTRIBUTION STATEMENT (of the abstract entered in Block 20, if different from Report)

18. SUPPLEMENTARY NOTES

19. KEY WORDS (Continue on reverse side if necessary and identify by block number)

Lithium-Boride	NMR
X-ray	Neutron
Crystal structure	EPR
Metallic Alloy	

20. ABSTRACT (Continue on reverse side if necessary and identify by block number)

A study has been made of the crystal structure of Li_5B_4 by X-ray, neutron powder diffraction techniques and NMR (nuclear magnetic resonance) measurements. The crystal structure thus determined is rhombohedral (R3) in its short-range ordered state and bcc (I23) in its statistically disordered (long-range) state.

The boron atomic arrangement consists of a coplanar triangular cluster of four boron atoms which are situated at the vertices and the center of the triangle. This boron atomic arrangement has no precedent either in metal-borides

DD FORM 1 JAN 73 1473 EDITION OF 1 NOV 65 IS OBSOLETE S/N 0102-014-6601

UNCLASSIFIED 391 596

SECURITY CLASSIFICATION OF THIS PAGE (When Data Entered)

or boron-hydrides. There is a strong indication that: 1) electrons on the boron atoms at the vertices are partially transferred (approx. 1.3 electrons) to the boron atom at the center of the triangle in Li_5B_4; and 2) the amount of electron transfer increases with temperature rise.

Lithium atoms, on the other hand, cluster in a bitetrahedral form (two tetrahedrons sharing a common face) with five lithium atoms occupying the vertices. This lithium atomic arrangement is in part similar to the hexagonal structure of lithium at low temperature.

NSWC/WOL/TR 77-84 22 June 1977

THE CRYSTAL STRUCTURE STUDY OF Li_5B_4

The research work reported herein was carried out during FY 76 and 77 in the Materials Division within the Research and Technology Department at the White Oak Laboratory under the guidance of Dr. Frederick E. Wang. Portion of the work pertaining to the Nuclear Magnetic Resonance study was carried out by Dr. Lawrence H. Bennett of the Institute for Materials Research at the National Bureau of Standards, Washington, D. C.

The project was sponsored exclusively by the Metallurgy Department of the Office of Naval Research under the contract number N00014-7TWR-T0030.

J. R. Dixon

J. R. DIXON
By direction

TABLE OF CONTENTS

TABLES

FIGURES

FIGURES (Cont.)

INTRODUCTION

Little is known about the phase equilibrium diagram of the Li-B system (Hansen & Anderko, 1958[1]; Elliot, 1965[2]; Shunk, 1969[3]; Handbook of Binary Metallic Systems, 1966[4]) as of this writing. Although several early attempts were made (Andrieux & Barbetti, 1932[5]; Markovskii & Kondrashev, 1957[6]; Moissan, 1892[7]) to prepare borides of alkali metals, it was not unitl 1963 that the existence of NaB_6 was established (Hagenmueller, 1963[8]); and a year later, LiB_4 was claimed in a French patent (French Patent, 1965[9]). On the other hand, the existence of LiB_6 was suggested (Kiessling, 1950[10]) and more recently confirmed (Rupp & Hodges, 1973[11]) experimentally. The compounds, LiB_2 and LiB_6, have been prepared under pressure and at temperatures in excess of 1400°C (Schimdt, 1976[12]). It also has been reported (Secrist & Childs, 1962[13]; 1967[14]) that a compound exists in the Li-B system at about 32 at.% Li. The compounds identified thus far in the Li-B system are all blackish powders except LiB_2 and LiB_6 which are reported to be golden-yellow and bluish-black (Schmidt, 1976[12]) in appearance respectively. However, mechanically they are all brittle and stable in air.

1. Hansen, M. and Anderko, K., "Constitution of Binary Alloys," McGraw-Hill Book Company, 1958.
2. Elliott, R. P., "Constitution of Binary Alloys, First Supplement," McGraw-Hill Book Company, 1965.
3. Shunk, F. A., "Constitution of Binary Alloys, Second Supplement," McGraw-Hill Book Company, 1969.
4. Handbook of Binary Metallic Systems, Translated from Russian by Schmorak, J., U.S. Department of Commerce, 1966.
5. Andrieux, J. L. and Barbetti, B., Compt.rend, 194, 1573; 1932.
6. Markovskii, L. Ya. and Kondrashev, Yu. D., Zhur. Neorg. Kim. 2, 34, 1957.
7. Moissan H., Compt.rend, 114, 319; 1892.
8. Hangenmueller, P., Compt.rend, 257, 1294; 1963.
9. Electroschmelzwerk Kempten G. m.B.H., French Patent No. 1,461,878; 1965.
10. Kiessling, R., Acta Chem. Scand. 4, 209; 1950.
11. Rupp, L.W., Jr. and Hodges, D. J., J.Phys.Chem.Sol 35, 617; 1973.
12. Schmidt, P. H., Private Communication (Bell Telephone Laboratory Murrey Hill, New Jersey) 1976.
13. Secrist, D.R. and Childs, W.J., US AEC TID-17149; US AEC KAPL-2182, 1962.
14. Secrist, D. R., J. Am Cer. Soc. 50, 520; 1967.

The Li_5B_4 compound-alloy studied here is dramatically different from those previously investigated in that it is ductile, malleable and has a metallic luster similar to that of lithium metal. The compound-alloy is susceptible to chemical attack by air as is lithium metal, although the reaction is somewhat less intense. In fact, the electro-chemical potential of the lithium-rich Li_5B_4 compound-alloy has been shown to be quite close to that of Li metal (James and DeVries[15]). Nevertheless, the melting temperature of Li_5B_4 is in the neighborhood of 1000°C compared to 182°C for Li metal. The electrical conductivity characteristic of the compound-alloy is metallic with a conductivity at R.T. (room temperature) in the range, $\approx 7 \times 10^6$ $(\Omega m)^{-1}$ (Mitchell and Sutula, 1977[16]).

EXPERIMENTAL

Alloy Preparation

The Li-B alloy specimens employed in this investigation were prepared in an inert atmosphere glove box equipped with a high capacity recirculating gas purification system. The system dynamically removes oxygen, moisture and nitrogen impurities from the helium gas such that the concentration of each of the impurities is less than one ppm. Crystalline boron (99.0%) from Kawecki Berylco and lithium (99.97%) from Foote Mineral Company were utilized in alloying. The lot of boron used contained 0.5 wt.% C, 0.14 wt.% Fe, 0.01 wt.% Si, and 0.09 wt.% O as principal impurities. The principal impurities in the lithium were 0.[illegible] wt.% Na, 0.006 wt.% Fe. Composition monitoring was accomplished principally by determining weight loss following alloy preparation. The weight of the final alloy varied from the initial weights by no more than 1%. The detailed procedure for the preparation of these Li-B alloys will be reported elsewhere (Wang, 1977[17]). The crystal structure of Li_5B_4 reported here has been investigated by a combination of X-ray, neutron diffraction techniques, and NMR (nuclear magnetic resonance) measurements. The experimental techniques entailed in each of these three disciplines are described below.

X-ray and Neutron Diffraction

Flat surfaced specimens for X-ray diffraction were prepared by machining the ends of a cylindrical shaped alloy (25mm dia. X 50mm length) in the glove box. The X-ray powder data were obtained with a Norelco diffractometer using Cu Kα (Ni filtered) radiation with

15. James, S. R. and DeVries, L. E., J. Elec. Chem. Soc. 123, 321; 1976.
16. Mitchell, M. A. and Sutula, R. A., to be published (Naval Surface Weapons Center, White Oak, Silver Spring, MD 20910); 1977.
17. Wang, F. E., to be published (Naval Surface Weapons Center, White Oak, Silver Spring, MD 20910); 1977.

specimens protected by a thin layer of oil. The fact that powder patterns thus obtained contain no oxidized material was confirmed by comparing them with those obtained from samples deliberately oxidized. Diffraction data were taken on both ends to insure homogeneity. While the "powder patterns" obtained from samples both in bulk and in powder form showed no preferred orientation for the Li-B compounds, a preferred orientation in bulk form is detected for Li metal as shown in Figure 1. The low temperature (approx. -180°C) data was obtained by blowing nitrogen vapor onto the surface of specimen whereas the 82°C data was obtained by circulating hot water through an enclosure which was in direct contact with the specimen.

For neutron diffraction, the flat specimen, also prepared in a glove box, was encapsulated in a Ti-Zr alloy which contributes no extra reflections (Sidhu, Heaton, and Mueller, 1959[18]). The intensities were obtained by an electronic integration which includes the height as well as the width of the peaks. The μT value used for the absorption correction was obtained experimentally by comparing the electronic counts obtained from the sample plus the sample-holder with those from the sample-holder alone.

NMR (Nuclear Magnetic Resonance)

For the NMR experiments, fine particles (~ 100 micron) were prepared under water-free paraffin oil in a glove box using a powder maker (Howling and Hoskins, 1965[19]) equipped with a fast spinning, diamond-studded end mill. A commercial wide-line NMR spectrometer, equipped with a 12" magnet and capable of generating magnetic fields in the range 600 - 17,000 Gauss, was used. Signals were accumulated on a multichannel analyzer for recording (METALS, 1973[20]). Because of the extreme ductility associated with the alloys with Li content greater than 60 at.% Li, the NMR data reported are limited to compositions from 42 to 60 at.% Li. Most of the measurements were made at R.T. Low temperature measurements were made using liquid-N_2 or liquid-freon in an insert type dewar.

CRYSTAL STRUCTURE STUDY

X-ray Diffraction

The X-ray powder diffraction patterns obtained at R.T. for lithium-boron compositions in the range 40 to 80 at.% Li are summarized in Figure 1. Analysis of these patterns indicates the existence of at least two intermediate phases within the composition range. The presence of Li metal, based on the observation of the 110 and 220 reflections (2θ = 36.1 and 76.57° for an a = 3.5 Å cubic cell), is

18. Sidhu, F. S., Heaton, L. and Mueller, M. H., J. Appl. Phys. 30, 1323; 1959.
19. Howling D. H. and Hoskins, J. M., Rev. Sci. Inst. 36, 400; 1965.
20. METALS, Edited by Bunshah, R. F., John Wiley & Sons, 1973.

detected only in the 80, 70, and 60 at.% Li compositions; whereas, the boron-rich intermediate phase, represented by two lines at 2θ = 12.2 and 20.9°, appears only in the 50 and 40 at.% Li compositions. Thus, the Li-rich phase, one of the two intermediate phases, is presumed to have a composition of about 55 at.% Li. This conclusion is supported by the diffraction pattern of 55 at.% Li shown in Figure 2, in which neither the Li nor the B-rich phase is present. This report is concerned with the studies made and the conclusions reached on the crystal structure of this Li-rich phase.

Most of the 9 diffraction lines (Figure 2) representing the 55 at.% Li phase can be indexed using cubic cells of three different dimensions, as shown in Table 1. Efforts were also made to index the 9 lines in systems other than cubic but they yielded no good agreement. The a = 7.0 Å cell was eliminated from further consideration because it does not account for the line at 2θ = 71.48°. The a = 4.93 Å cell is the only one that accounts for all 9 observed lines. However, closer inspection of the diffraction patterns (Figure 1) shows that three (2θ = 40.8, 62.31, and 79.94°) of the 9 lines attributed to the 55 at.% Li phase shift by as much as one degree (in their 2θ) in going from 40 to 80 at.% Li (See Table 2). Particularly noteworthy is the absence of any corresponding shifts in the remaining six lines over the same composition range. Therefore, these three lines cannot belong to the same diffraction pattern even though they happen to be indexible by the a = 4.93 Å cell. This contention is further enhanced by the fact that the intensities of these three anomalous lines do not increase or decrease with change of composition in the same manner as the other six lines (See Figure 1).

The three anomalous lines described above correspond to HKL = 210, 311, and 410 of the a = 4.93 Å cell and are all of the H+K+L = 2n+1 type. The remaining six lines are all of the H+K+L = 2n type and indicate bcc symmetry. It is interesting to note that the three lines also happen to be those indexible by the a = 6.06 Å cell, which makes this another possible choice. However, this choice was regarded as unlikely because the remaining reflections do not show bcc or fcc extinction and more importantly, a Patterson synthesis based on the a = 6.06 Å showed unreasonable interatomic distances. Thus, the a = 4.93 Å was chosen for further structural analysis.

Because of the sharp decline in diffraction intensity with increasing 2θ (for example, compare the 110 with the 220 reflection of the a = 4.93 Å cell), it would appear that the available data are severely limited by thermal vibration. In order to overcome this difficulty, a diffraction pattern was obtained at liquid-N_2 temperature (approx. -180°C). Contrary to our expectation, the diffraction pattern (Figure 2) shows not only no increase in the intensities at high angles but also an overall decline in the intensities. In addition, the peaks are somewhat less defined than that observed at R.T. This may mean that the compound is in a metastable state which becomes even less stable at low temperature, that is, it is more stable at high temperatures. This trend is confirmed by a diffraction pattern

obtained at 82°C from the same sample (as shown in Figure 2). While there is no significant difference between the high angle region of this pattern and the one at R.T., the first peak, $2\theta = 25.40$, at 82°C is definitely more intense than that observed at R.T. These observations are entirely reversible in a given sample and tend to confirm the contention that the compound is actually metastable. However, they also demonstrate the futility of obtaining more and better data by lowering the temperature.

Patterson Synthesis

A Patterson synthesis based on the six diffraction lines listed in Table 2 (using the $a = 4.93$ Å cubic cell) shows six symmetry independent peaks, (a) through (f), as shown in Figure 3. Considering the peak positions alone, all the Patterson peaks except peak (e) at $u = v = w = 1/4$ can be accounted for by two units of a tetrahedral cluster of four atoms related by bcc symmetry (i.e., 0, 0, 0 and 1/2, 1/2, 1/2). Referring to Figure 4, the atomic positions are:

ATOM	X	Y	Z	
(1)	x	x	x	with x = .175
(2)	-x	-x	x	plus 1/2, 1/2, 1/2, leads to:
(3)	x	-x	-x	(1)', (2)', (3)', and (4)'.
(4)	-x	x	-x	

The Patterson peak, (e), can be satisfied by having additional atoms in the following positions which also conform to bcc symmetry:

ATOM	X	Y	Z	
$(\bar{1})$	x	x	x	with x = .925
$(\bar{2})$	-x	-x	x	plus 1/2, 1/2, 1/2, leads to:
$(\bar{3})$	x	-x	-x	$(\bar{1})'$, $(\bar{2})'$, $(\bar{3})'$, and $(\bar{4})'$.
$(\bar{4})$	-x	x	-x	

It is clear that simultaneous occupation of all these positions is impossible because the interpositional distances (within each tetrahedral cluster) are too close to accomodate either Li or B. The determination of which positions are occupied and by which type of atoms was made based on the following considerations and limitations:

(a) The positions chosen and the atoms (Li or B) placed in these positions should be such that the interpositional distances found must agree with the Li and B atomic radii ($R_{Li} \simeq 1.5$ Å, $R_B \simeq .75$ Å) within 10 to 15%.

(b) The chemical compositions of the compound should have an atomic ratio, Li/B, of about 55/45.

(c) The crystal structure thus chosen must have cubic symmetry or a subgroup of such symmetry. The allowance of a subgroup is based on the consideration that the available data are from powder and not from single crystals.

(d) The theoretical density must be in reasonable agreement with that observed.

In Figure 5, we show a structure (projected onto the x-y plane) which conforms to all the above described restrictions. In this structure, the compound has the chemical formula, Li_5B_4 (55.55 at.% Li), and a psuedo-cubic rhombohedral symmetry with a = 4.93 Å and $\alpha = 90°$. As shown in Figure 6, the interatomic distances are also in reasonable agreement. The calculated density of 1.06 gm/cc is in fair agreement with the experimental value of 1.00 ($\pm$ .02) gm/cc (at 55 at.% Li as prepared composition), considering that the alloy has a persistent fractional presence of another compound (represented by the three anomalous lines) in the alloy, plus the inherent micro-cavities in a cast-alloy.

It should be noted that a triangular cluster of 4 B atoms and a triangular cluster of 3 Li atoms are essentially identical in size (See Figure 6a). The basic feature of this structure is a chain in the [111] direction made up of Li atoms (Li-1, Li-5) sandwiched between B and Li clusters (Figure 6b). In view of the fact that the data were obtained from powder patterns (not from single crystals), this choice of rhombohedral symmetry is theoretically acceptable. However, internal disorder, based on this rhombohedral structure, should also be considered. Such disorder can arise in two ways. The first may be classified as "stacking faults" due to an interchange of B and Li clusters. This can occur because they are essentially identical in size and probably have similar electronic structures. The second type of disorder may result from twinning between micro-sized rhombohedral domains so as to generate a higher symmetry (i.e., cubic). The probability of such twinning is expected to be high because the rhombohedral structure has an $\alpha = 90°$ (pseudo-cubic). A combination of these two types of disorder can result in bcc symmetry. The crystallographic data thus obtained for both the rhombohedral and disordered rhombohedral (cubic) structures are as follows:

Rhombonedral (R3m = C_{3v}^5; trigonal)

3(Li)	x,x,z; z,x,x; x,z,x;	(x = .325; z = -.325)
1(Li)	x,x,x;	(x = .175)
1(Li)	x,x,x;	(x = .675)
3(B)	x,x,z; z,x,x; x,z,x;	(x = -.175; z = .175)
1(B)	x,x,x;	(x = .925)

Disordered Rhombohedral (I23 = T^3; bcc)

8(f_1)	x,x,x; x,$\bar{x}$,$\bar{x}$; $\bar{x}$,x,$\bar{x}$ $\bar{x}$,$\bar{x}$,x;	(x = .175)
8(f_2)	Same as above;	(x = .925)

Where $f_1 = (5f_{Li} + 3f_B)/8 = 3.75$ electrons

$f_2 = (f_B)/8 = .625$ electrons.

In order to determine a correct choice between the two possibilities, theoretical Patterson peaks were generated for the two structures.

Patterson Peaks for R3m

It should be noted that in this calculation, an average value between the two distinct directions (parallel vs. perpendicular to the rhombohedral axis) is taken to simulate the powder data.

#	u	v	w	Interaction	Peak Height
(a)	0,	0,	0;	5(Li-Li)+4(B-B)	145
(b)	.35,	.35,	.35;	[(Li-B)+2(Li-Li)+(B-B)]/2	29
(c)	.50,	.17,	.17;	[(Li-Li)+3(Li-B)]/2	27
(d)	.11,	.11,	.21;	(B-B)	25
(e)	.25,	.25,	.25;	2(Li-B)	30
(f)	.50,	.50,	.50;	2[3(Li-B)+(Li-Li)]	108

Patterson Peaks for I23

Since the four atoms with f_2 scattering factor are spatially very close to one another with respect to the atoms (Li-1, Li-5) with the f_1 scattering factor, all four are considered to contribute to the peak, (e), - See Figure 3.

#	u	v	w	Interaction	Peak Height
(a)	0,	0,	0;	$2[4(f_1-f_2)+4(f_1-f_2)]$	116.0
(b)	.35,	.35,	.35;	$2(f_1-f_1)$	28.1
(c)	.50,	.17,	.17;	$2(f_1-f_1)$	28.1
(d)	.11,	.11,	.21;	$2(f_1-f_2)$	4.7
(e)	.25,	.25,	.25;	$4[4(f_1-f_2)]$	37.5
(f)	.50,	.50,	.50;	$2[4(f_1-f_1)+4(f_2-f_2)]$	116.0

The heights of these theoretical Patterson peaks are compared with the observed peaks in Table 3. It is clear that the disordered rhombohedral (I23) structure is the better choice.

Neutron Diffraction

Since in neutron diffraction the nucleus scattering length of B(boron) is positive (b_B = +.534) and Li is negative (b_{Li} = -.214), simultaneous agreement between the observed and calculated intensities in both X-ray and neutron diffraction is not only ideal but also essential in checking the credibility of the proposed I23 structure. Because of the high neutron mass absorption coefficient of the ^{10}B isotope (σ_n = 3836 barns) compared to ^{11}B (σ_n = 0.005 barns), ^{11}B isotope was used in forming the Li_5B_4 alloy for collecting the final neutron diffraction data (Table 5). Neutron diffraction data were also obtained from Li_5B_4 made of "natural" boron (mixture of ^{10}B and ^{11}B) to check whether there were any characteristic differences between the patterns from ^{11}B and from "natural" boron. We observed no differences aside from the expected absorption difference. As shown in Table 4, the neutron diffraction powder pattern is also indexible on the a = 4.93 Å cubic cell. The H+K+L = 2n reflections observed (and unobserved) by neutron diffraction are essentially

those observed (and unobserved) by X-ray diffraction. It is of great interest to note that the three anomalous reflections (indexible as H+K+L = 2n+1 but were deleted from consideration because of their independent shifts in 2θ angle as a function of composition) in the X-ray data are totally absent from the neutron diffraction data. This tends to lend additional support to the correctness of deleting them from consideration as part of the a = 4.93 Å cell data.

Structural Refinement

Based on the X-ray data, initial refinement was made as follows. In the disordered I23 structure, there are at least three parameters to be determined and refined: two independent atomic coordinates (x_1, x_2) plus an isotropic temperature factor. Since there are only six independent experimental data available, the three parameters cannot be refined in a standard manner (i.e., least squares refinement). As an alternative, structure factors were calculated as a function of atomic coordinates in the vicinity of x_1 = .175 and x_2 = .925 (obtained in the Patterson synthesis). By combining these structure factors and multiplying by Lp (Lorentz-polarization), M (multiplicity), B (isotropic temperature factor) and the averaged atomic scattering factors, f_1, f_2, intensities were calculated. Absorption was not considered because both Li and B have low atomic numbers.

Based on the parameters used in X-ray, intensities were calculated for neutron diffraction and compared with those observed. In these calculations, the neutron scattering lengths, b (Li) = -.214, b(^{11}B) = +.65 and an absorption correction, μT = .59 were used. The best agreement for both the X-ray and neutron diffraction data comes from x_1 = .175, x_2 = .985 and 2B = 7 as shown in Table 5. While the agreements for both the X-ray and neutron are reasonable, they are far from perfect, particularly the 200 of X-ray and the 211(330) of neutron diffractions. However, these minor less-than-perfect matches, we believe, are due to a number of factors that are impossible to correct for unless more data become available. These are:

a) The short-range triangular atomic arrangements (Fig. 6) suggest a strong inisotropic thermal vibrations and subsequently inisotropic temperature factors.

b) Metastable nature of the compound as exhibited in the X-ray pattern as a function of temperature (Fig. 2) suggests a possible anomalous temperature factor.

c) The triangular cluster of 3 lithium atoms and 4 boron atoms (Fig. 6) cannot be exactly the same size (see Discussion). As a result, the long-range statistical disorder involves replacement disorder as well as a fraction of displacement disorder. Nevertheless, the calculated intensities are based on the replacement alone (with the coordinates unchanged).

In view of these limitations and shortcomings the agreements between the calculated and observed for both the X-ray and neutron diffractions are therefore considered good.

We now direct our attention to the X-ray diffraction pattern as a function of temperature in which the 110 peak increased its intensity independently with the temperature rise. While only the liquid-N_2, R.T. and 82°C patterns are shown in Fig. 2, there are a number of patterns taken in between R.T. and 82°C that indicates the 110 peak intensity increase to be roughly proportional to the temperature rise. We have found this anomalous 110 intensity increase can be explained by assuming partial electron transfer from the corner boron to the center boron atoms. This is demonstrated in Table 6 in which the calculated X-ray diffraction pattern is given as a function of such an electron transfer. The 110 intensity is the only one that remains strong (or if the other peak intensities were to remain at the same level, the 110 intensity will increase independently) with an increase in the electron transfer. This is to say that the partial electron transfer from the corner B atoms to the center B atom is enhanced with the temperature rise. If this temperature-dependent electron transfer interpretation is correct, the neutron diffraction, which is independent of the electron density distribution, should show no change as a function of temperature. This was experimentally confirmed by monitoring the peak height of the 110 reflection in neutron diffraction over a wide temperature range. As shown below, no change in the 110 peak height (within the experimental deviation) as a function of temperature is observed.

Temp.(°C)	110 Peak Height
25	93 (± 3)
74	96 (± 3)
215	92 (± 3)
320	94 (± 3)
400	96 (± 6)
442	94 (± 6)
540	91 (± 6)
690	99 (± 6)
805	86 (± 6)

It is tempting to speculate at this point, (because $x_2 = .985$ is very close to 1 and transfer of electrons from the corner B atoms to the center B atom is tantamount to transferring the corner B into Li) that the structure may be actually I23 with 8 Li atoms occupying 8(c) and 2 B atoms occupying 2(a) positions. However, such a structure yields no agreement with either the neutron, NMR data or the composition requirement, the measured density of the compound-alloy, and therefore is not acceptable.

Efforts Made in Single Crystal Growth

A number of attempts were made to grow single crystals of Li_5B_4 compound-alloy for X-ray diffraction studies. These attempts included:

a) Growth of the crystals directly from the alloy melt. In this approach, 1/2 mm o.d. steel wire was dipped into the melt and slowly pulled away from the melt. This resulted in the alloy sticking to the wires' tip in the form of tiny beads. The wire with beads was then annealed for a prolonged period (4 to 48 hrs.) at various temperatures.

b) Zone-refining by electron beam. Liquid alloy was introduced into steel tubing of 2 mm o.d. and 1.5 mm i.d. Upon solidification, the ends of the tubing were pinched off to form a sealed tube filled with the alloy. The electron beam was then repeatedly passed over the midsection (approx. 5 cm in length) for as many as 20 times at the speed of 2 cm per hour.

c) Strain-anneal method. Bulk alloy was mechanically pressed (rolled) into a sheet, a fraction of a millimeter thick. The sheet was then sliced with sharp knife into rectangular rods (approx. .5 X .5 X 8 mm). The rods were then annealed for a prolonged period (4 to 48 hrs.) at various temperatures. In some cases, the annealed rod was reworked mechanically and reannealed.

d) Modified strain-anneal method (Wang, et.al., 1964[21]). In this approach, the annealing was accomplished by electrical resistance heating. Thus, electric current was passed through the rods, prepared as in the strain-anneal method. Because of the high conductivity associated with the alloy, resistance heating required a large current. This made fine control of electric current fluctuations extremely difficult if not outright impossible.

None of the above approaches yielded single crystals of Li_5B_4. In a number of cases Li single crystals (Figure 7) were obtained in the process but no single crystals of Li_5B_4 were obtained. The difficulty of growing single crystals is perhaps associated with the metastable nature of the compound-alloy as described above.

NMR (Nuclear Magnetic Resonance)

Large number of both ^7Li and ^{11}B nuclear magnetic resonance measurements were made on the Li-B alloys of differing compositions. A few typical spectra are shown in Figures 8-11. Most of the measurements were made at R.T., but some were made at 77°K. The only

21. Wang, F. E., Syeles, A. M., Clark, W. L., and Buehler, W. J., J. Appl. Phys., 35, 3620, (1964).

significant effects of temperature were found for the ^{7}Li NMR in alloys containing less than 55 at.% Li, where the linewidths varied with temperature. A typical result is shown in Figure 11. NMR measurements were made at varying frequencies, modulation amplitudes, rf levels, sweep rates, sweep amplitudes, and in both absorption and dispersion modes (Weisman, Swartzendruber, and Bennett, 1973[22]).

There were no obvious systematic differences in the ^{11}B NMR for any alloy, and thus the local electronic configuration sampled by the boron is not greatly altered by alloying. Spectra for four compositions are shown in Figure 8. The structure is similar in each of the spectra shown. The central ($1/2 \longleftrightarrow -1/2$) peak has a Knight shift near 0%. The center of the satellite ($3/2 \longleftrightarrow 1/2$, $-3/2 \longleftrightarrow -1/2$) peaks appears to be shifted to negative Knight shifts. The shape of these spectra depends critically on the spectrometer settings and is not to be confused with second order quardupole effects. Measurements at half the frequency (8 MHz) demonstrate the absence of second-order effects. The best preliminary estimate of the lineshape is that there are two local boron environments, each with first order quadrupole effects, having different Knight shifts and saturation behavior. Additional broadening is present due to defect structure.

In contrast to the ^{11}B NMR, the ^{7}Li resonances were dramatically different as a function of composition (see Figure 9). For B compositions less than Li_5B_4, the ^{7}Li NMR was similar to its resonance in Li metal. For B compositions above Li_5B_4, the ^{7}Li NMR was quite different, with a near zero (0.007 ± 0.003%) Knight shift, observable quadrupole effects, and temperature independent results.

For B concentrations below Li_5B_4, the ^{7}Li Knight shift was 0.0251 ± 0.0005%, very near to the Knight shift in Li metal (Carter, Bennett, and Kahan, 1977[23]). The linewidth of pure Li is known to be diffusion-narrowed at R.T. limiting instrumental resolution. Our measurement shows 0.35 G, including modulation (0.25) broadening. The Li-B alloy, however, shows definitely broader lines, about 0.8 G. At Liquid-N_2 temperature, the linewidths of Li metal and of the Li-B alloys are equal (about 5.5 G). This is slightly below the literature value (about 6.2 G) for Li metal. "Rough" measurements made between 77°K and 300°K seem to indicate that the line narrowing in the alloy occurs near the same temperature as in Li metal, as indicated in Figure 10. This rapid diffusion of Li in the Li-B alloys makes these alloys promising candidates for battery electrodes.

22. Weisman, I. D., Swartzendruber, L. J. and Bennett, L. H., "Technique of Metals Research," Vol. VI, John Wiley & Sons, 1973.
23. Carter, G. C., Bennett, L. H., and Kahan, D. J., "Metallic Shifts in NMR," Progress in Mateirals Science, 20, Pergamon Press, (1977).

The ^7Li NMR in Li_5B_4 and higher boron composition showed no such line narrowing, but did display quadrupole effects. As an example, consider the spectrum of the high boron alloy shown in Figure 11. The central (1/2 $\longleftrightarrow$ -1/2) line is unsplit, but two distinct sets of ($\pm$ 3/2 $\longleftrightarrow \pm$ 1/2) quadrupole satellites are clearly resolved. Hence, there are two distinct Li sites in the Li_5B_4 compound and in alloys with higher boron contents.

The NMR results support several aspects of the crystal structure determination. The sharp change in the ^7Li resonance at Li_5B_4 indicates compound formation at this composition. Two different B environments and two different Li environments are observed. Local cubic symmetry is absent at any site. The fact that the local site symmetry of the B is the same in all the samples suggests an almost continuous change from bcc Li metal to an ordered Li-B structure. The Knight shift of the Li in the compound appears to be similar to LiAl, LiGa, and LiIn compounds (Bennett, 1966[24]), which are semimetals.

DISCUSSION

In summary, the Li_5B_4 crystal structure thus elucidated has two parts: the short-range vs. long-range structure. The short-range structure (R3m) has the support of NMR data, density and composition determinations whereas the long-range structure (I23) has the agreement of both the X-ray and neutron diffraction data. Without the short-range structure (R3m), NMR data which exhibits noncubic symmetry will be hardly justifiable (in view of the X-ray and neutron data). Reversely, the X-ray and neutron data which shows cubic symmetry will be equally difficult to justify without the long-range structure (I23). To be sure, in the absence of single crystal data, the crystal structure thus characterized cannot be considered absolutely correct. However, data from all three disciplines (X-ray, neutron, NMR) taken together yield rather convincing evidence in support of the structure. For example: a) there exists simultaneous agreement for both X-ray and neutron diffraction, b) since the unobserved reflections (which are calculated to be small) are also an agreement, the total number of independent agreements for a combined X-ray and neutron diffraction is 25 instead of 13 (actually observed) and c) the local arrangement of B and Li atoms thus elucidated from X-ray and neutron diffraction are in total agreement with the NMR finding.

Inasmuch as the coordinates, x_1, x_2 obtained are based on the statistically averaged values between the four B atom cluster and the three Li atom cluster (Figure 6), the interatomic distances between B atoms and between Li atoms cannot be determined uniquely.

24. Bennett, L. H., Phys. Rev., 150, 418 (1966).

However, based on the known atomic (metallic) radii of Li and B, one would conclude that the actual Li-Li interatomic distances in Li_5B_4 are somewhat larger than 2.44 Å. On the other hand, the B-B interatomic distances should be somewhat less than 1.41 Å. Thus, the approximate interatomic distances found in Li_5B_4 for Li and B are shorter than their respective interatomic distances (Li-Li = 3.04 Å, B-B = 1.58 Å) in their metallic states (Interatomic Distances, 1958[25]) by as much as 13-16%.

The four B atomic arrangement (coplanar triangle) is unique and has no precedent either among the metal-borides (International Symposium on Boron and Borides, 1976[26]) or among the boron-hydrides (Lipscomb, 1963[27]). Corresponding to this unique feature is the fact that the Li_5B_4 compound-alloy is totally metallic and dramatically different from other alkali borides investigated thus far in its physical characteristics, e.g., ductile, malleable and susceptible to chemical attack by air like metal. The five Li atom trigonal-bipyramid cluster, on the other hand, is reminiscent of the hexagonal structure of Li metal at low temperature (Barrett, 1956[28]).

The indication of partial electron transfer (among boron atoms) as a function of temperature, based on the X-ray and neutron data may not be unreasonable in that the "three-center" bond in boron-hydrides is known to distribute electrons unequally among the three centers (Switkes, Lipscomb & Newton, 1970[29]). Furthermore, experimentally since Li and B have atomic number of only 3 and 5, respectively, a transfer of a fraction of one electron constitutes a high percentage of electrons surrounding the atoms, and should be easily detected by X-ray diffraction.

As described above, the justification for deleting the three anomalous lines (observed in X-ray) is principally based on the observation of the independent shifts in 2θ and intensities of these three lines as a function of composition. This justification is further enhanced indirectly by the fact that the crystal structure thus arrived at - without these three anomalous lines - is in reasonable agreement with all the remaining observed data. Nevertheless, the origin of the three delected anomalous X-ray diffraction lines remains to be reconciled. The fact that the intensities of these three lines remain fairly constant even at 40 at.% Li (Figure 1) suggests that they may belong to a B-rich phase. This speculation, it is hoped, will be resolved in our continuing study of the B-rich phase. Concurrently, investigation of these compound-alloys by the EPR (electron paramagnetic spin resonance) is underway and should shed more light on these remaining questions in the near future.

25. Interatomic Distances, The Chem. Soc., London, Burlington House, W.1 (1958).
26. International Symposium on Boron and Borides, J. Less Comm. Met. Vol. 47 (1976).
27. Lipscomb, W. N., "Boron Hydrides," W. A. Benjamin, Inc. (1963).
28. Barrett, C. S., Acta Crystal. 9, 671 (1956).
29. Switkes, E., Lipscomb, W. N., and Newton, M. S., J. Am. Chem. Soc. 92, 3847 (1970).

ACKNOWLEDGEMENT

We are most grateful to Dr. Allen L. Bowman of the Los Alamos Scientific Laboratory for supplying us with the neutron diffraction data and the μT absorption correction. Thanks is also due Mr. Robert L. Parks of National Bureau of Standards for preparing NMR samples and the technical assistance rendered in the NMR measurements.

Table 1

OBSERVED		Cubic a = 7.0 Å		Cubic a = 4.93 Å		Cubic a = 6.06 Å	
2θ	I(rel.)	2θ	d(hkl)	2θ	d(hkl)	2θ	d(hkl)
25.40	100	25.44	3.50(200)	25.52	3.50(110)	25.44	3.50(111)
40.80	22	40.75	2.21(310)	40.87	2.21(210)	-	
44.86	65	44.87	2.02(222)	44.87	2.02(211)	44.87	2.02(300)
52.38	15	52.26	1.75(400)	52.43	1.74(220)	52.26	1.75(222)
62.31	12	62.22	1.49(332)	62.40	1.49(311)	-	
71.48	5	-		71.53	1.32(321)	71.31	1.32(421)
79.94	7	79.94	1.20(530) (433)	79.94	1.20(410) (322)	-	
82.96	14	82.77	1.16(600) (442)	83.01	1.15(411) (330)	82.77	1.16(511) (333)
99.86	9	99.51	1.01(444)	99.86	1.01(422)	99.41	1.01(600) (442)

Table 2

2θ(obs.)	d(obs.)	I(obs.)	HKL	2θ(cal.)	d(cal.)
		-	100	17.97	4.9360
25.40	3.5065	100	110	25.52	3.4997
		-	111	31.40	2.8498
		-	200	36.41	2.4668
(40.38-41.20)*		-	210	40.87	2.2079
44.86	2.0204	65	211	44.87	2.0200
52.38	1.7467	11	220	52.44	1.7451
		-	300	55.89	1.6450
			221	"	"
		-	310	59.23	1.5600
(61.90-62.61)*		-	311	62.40	1.4881
		-	222	65.52	1.4246
		-	320	68.56	1.3687
71.48	1.3198	5	321	71.53	1.3189
		-	400	77.34	1.2337
(79.70-80.42)*		-	410	79.94	1.1969
			322	"	"
82.96	1.1639	13	411	83.01	1.1632
			330	"	"
		-	331	85.83	1.1321
		-	420	88.63	1.1035
		-	421	91.42	1.0769
		-	332	94.22	1.0521
99.86	1.0074	9	422	99.81	1.0073

* The reflections which shifted its 2θ as a function of composition.

Table 3

	Observed		Rhombohedral(R3m)	bcc(I23)
#	Position	Rel.Ht.	Cal. - Obs.*	Cal. - Obs.*
(a)	u = 0 v = 0 w = 0	1000	145 - 145	116 - 116
(b)	u = .35 v = .35 w = 0	217	29 - 31	28 - 25
(c)	u = .50 v = .17 w = .17	217	27 - 31	28 - 25
(d)	u = .11 v = .11 w = .21	30	25 - 4.35	4.7 - 3.5
(e)	u = .25 v = .25 w = .25	270	30 - 39	37 - 31
(f)	u = .50 v = .50 w = .50	1000	108 - 145	116 - 116

* These values are obtained by scaling down the observed Relative heights with respect to the origin peak.

Table 4

2θ(obs.)	d(obs.)	I(obs.)	HKL	2θ(cal.)	d(cal.)
		-	100	13.30	4.9360
18.83	3.4906	100	110	18.84	3.4997
		-	111	23.13	2.8488
		-	200	26.76	2.4668
		-	210	30.00	2.2079
32.96	2.0127	12.4	211	32.93	2.0200
38.25	1.7438	23.3	220	38.20	1.7451
		-	300 221	40.63 "	1.6450 "
		-	310	42.93	1.5600
		-	311	45.13	1.4880
		-	222	47.23	1.4246
		-	320	49.33	1.3687
51.38	1.3185	27.9	321	51.33	1.3189
55.23	1.2331	-	400	55.32	1.2337
		-	410 330	57.00 "	1.1969 "
58.86	1.1621	15.3	411 330	58.80	1.1632
		-	331	60.60	1.1321
		-	420	62.33	1.1035
		-	421	64.07	1.0769
		-	332	65.73	1.0521
68.95	1.0091	5.8	422	69.06	1.0073
		-	500 430	70.70 "	.9870 "
72.39	.9669	13.6	510 431	72.33 "	.9678 "

Table 5

	X-ray(λ = 1.5417 Å)					Neutron(λ = 1.1422 Å)				
hkℓ	2θ	I_o	I_c	$M\|F_c\|^2$	K	2θ	I_o	I_c	$M\|F_c\|^2$	K'
110	25.40	100	100	19.8	5.05	18.83	100	100	18.9	5.29
200	36.41	-	18	9.1	1.98	26.76	-	4	.2	2.84
211	44.87	65	75	65.3	1.15	32.93	13	61	33.0	1.85
220	52.44	11	11	16.2	.68	38.20	23	24	24.1	.99
310	59.23	-	5	11.4	.44	42.93	-	4	2.9	.65
222	65.52	-	2	.1	.31	47.23	-	4	7.5	.49
321	71.53	5	8	34.2	.24	51.33	28	33	79.9	.41
400	77.34	-	2	.7	.18	55.32	-	4	1.5	.34
411	83.01	13	15	100.0	.15	58.80	15	27	100.0	.27
330	"					"				
420	88.63	-	2	8.0	.13	62.33	-	6	31.5	.21
332	94.22	-	2	13.6	.12	65.73	-	4	.4	.18
422	99.81	9	3	26.4	.11	69.06	6	5	30.4	.16
510	----------					72.33	14	13	96.7	.13

M(multiplicity factor from I23) is common to both the X-ray and neutron diffraction.

S(temperature factor) = $\exp(-2B \cdot \sin^2\theta/\lambda^2)$ is applied to both the X-ray and neutron diffraction with B =3 common to both.

For X-ray, $I_c = K \cdot M \cdot |F_c|^2$, where $K = N \cdot Lp \cdot S$

N(normalization factor) = .1477
Lp(Lorentz-polarization) = $(1+\cos^2 2\theta)/\sin^2\theta \cdot \cos\theta$

For neutron, $I_c = K' \cdot M \cdot F_c$, where $K' = N \cdot A \cdot L \cdot S$

N(normalization factor) = 2.6596
A(absorption correction) = $\exp[-\mu T \cdot \sec\theta]$
with μT = .59
L(Lorentz factor) = $1/\sin^2 2\theta$

Table 6

CALCULATED INTENSITY(X-RAY) AS A FUNCTION OF ELECTRON TRANSFER

	hkℓ	110	200	211	220	310	222	321	400	411	420	332	422
	2θ	25.5	36.4	44.9	52.4	59.2	65.5	71.5	77.3	83.0	88.6	94.2	99.8
	I_o	100	-	65	11	-	-	5	-	13	-	-	9
Electron Transfer	0	100	18	75	11	5.5	<2	8.5	<2	15	<2	<2	2.4
	.1	100	16	73	11	4.8	<2	8.3	<2	15	<2	<2	2.3
	.2	100	14	70	11	4.2	<2	8.2	<1	15	<2	<1	2.3
	.3	100	13	68	11	4.0	<2	8.2	<1	14	<2	<1	2.2
	.4	100	12	66	11	3.6	<2	8.2	<1	14	<2	<1	2.1
	.5	100	11	62	11	3.2	<2	8.1	0	13	<2	<1	2.0
	.6	100	10	59	11	2.8	<1	8.0	0	12	<2	<1	1.9
	.7	100	9	56	11	2.3	<1	8.0	0	12	<2	0	1.8
	.8	100	8	53	10	1.8	<1	8.0	0	11	<1	0	1.7
	.9	100	7	51	10	1.6	<1	7.9	0	11	<1	0	1.6
	1.0	100	6	48	10	1.4	<1	7.9	0	10	<1	0	1.5
	1.1	100	5	46	10	1.2	0	7.9	0	10	0	0	1.4
	1.2	100	4	44	9	1.0	0	7.9	0	9	0	0	1.4
	1.3	100	3	42	9	.8	0	7.9	0	9	0	0	1.3

Fig. 1


X-ray Powder Pattern (Cu Kα)
40 at % Li(B)
50 at. % Li(B)
60 at. % Li(B)
70 at. % Li(B)
80 at. % Li(B)
2θ

Fig. 2

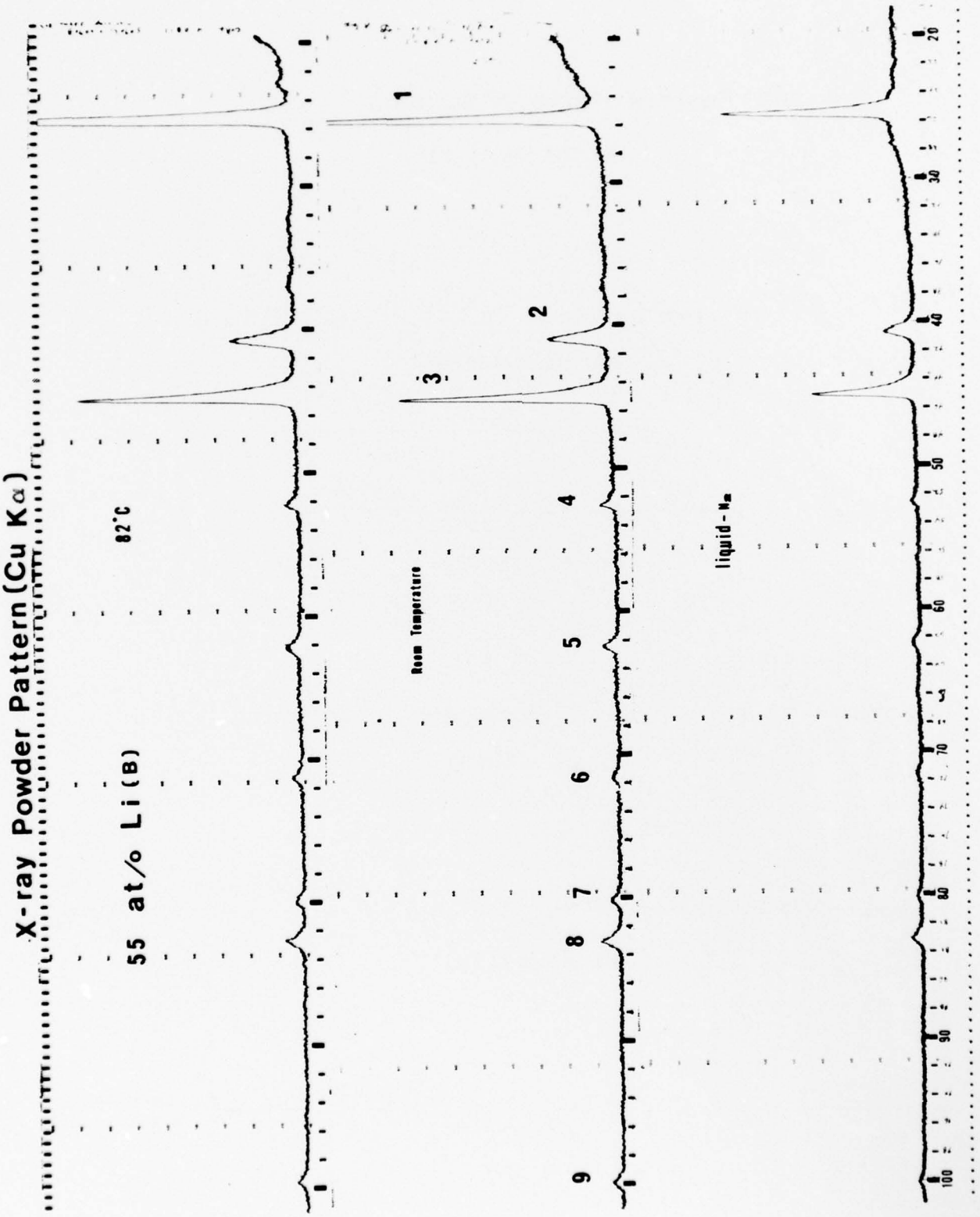
X-ray Powder Pattern (Cu Kα)
55 at/o Li (B)
82°C
Room Temperature
liquid-Na
1
2
3
4
5
6
7
8
9

Fig. 3

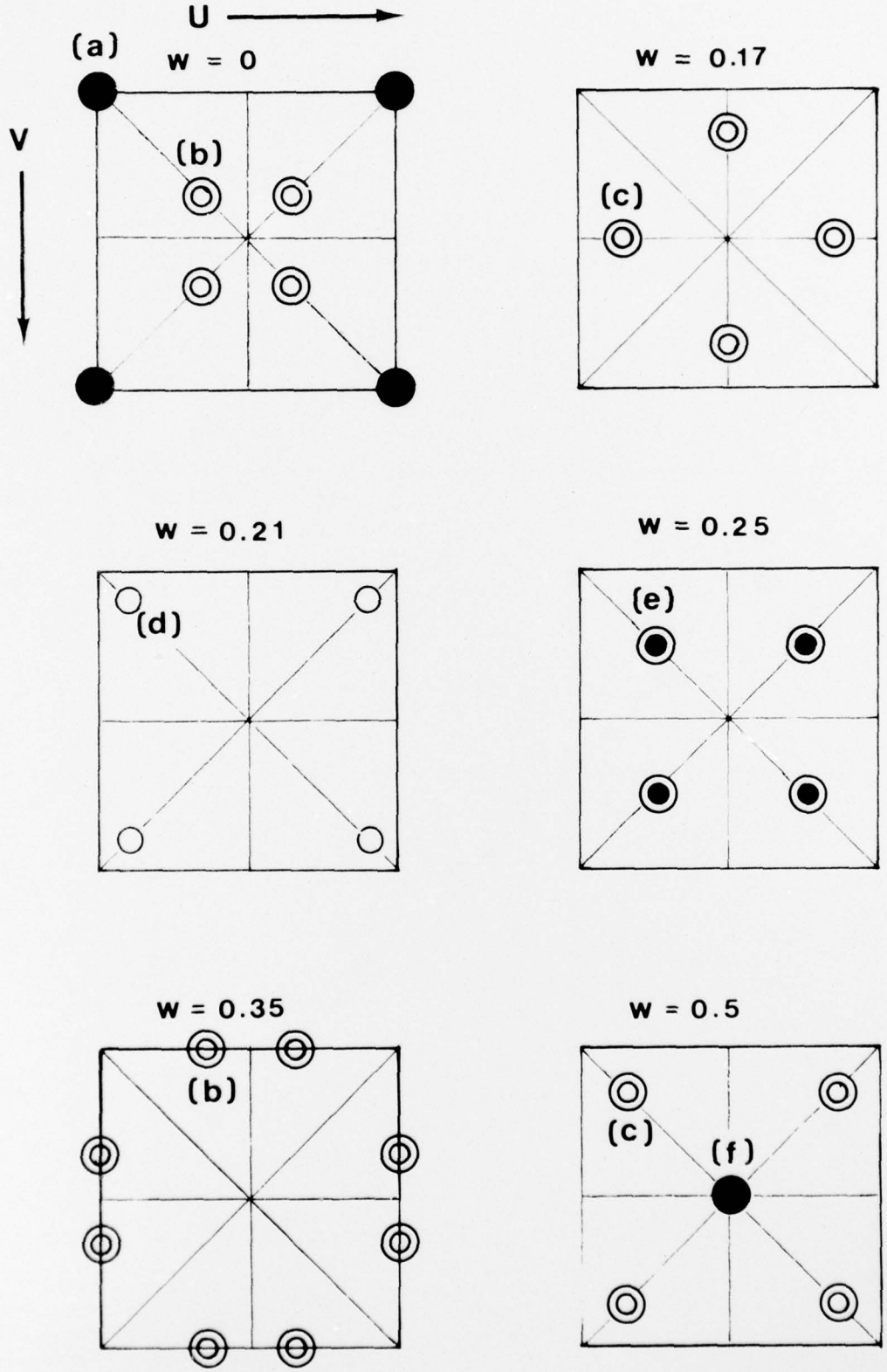

Fig. 4

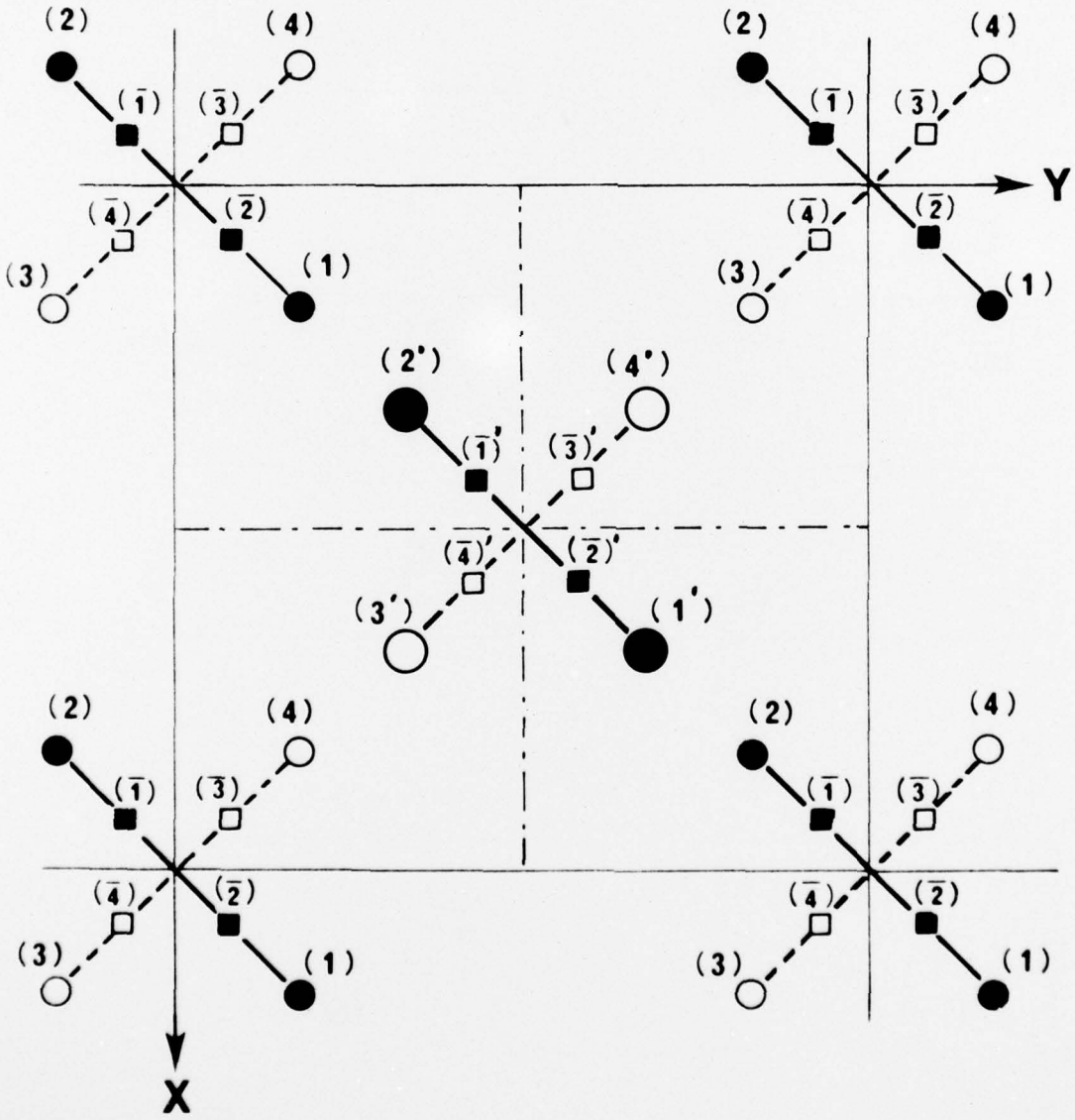

Fig. 5

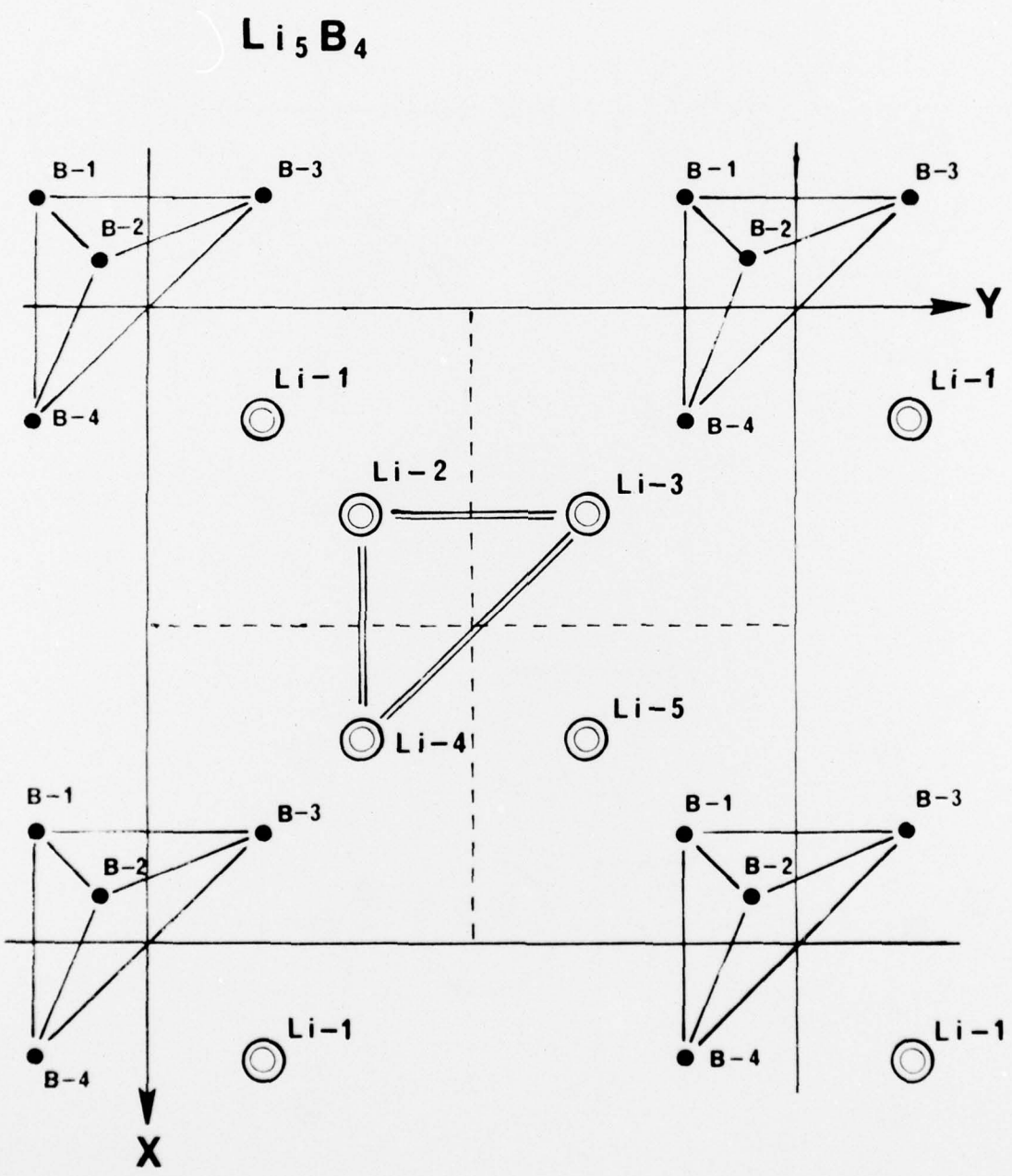

Fig. 6

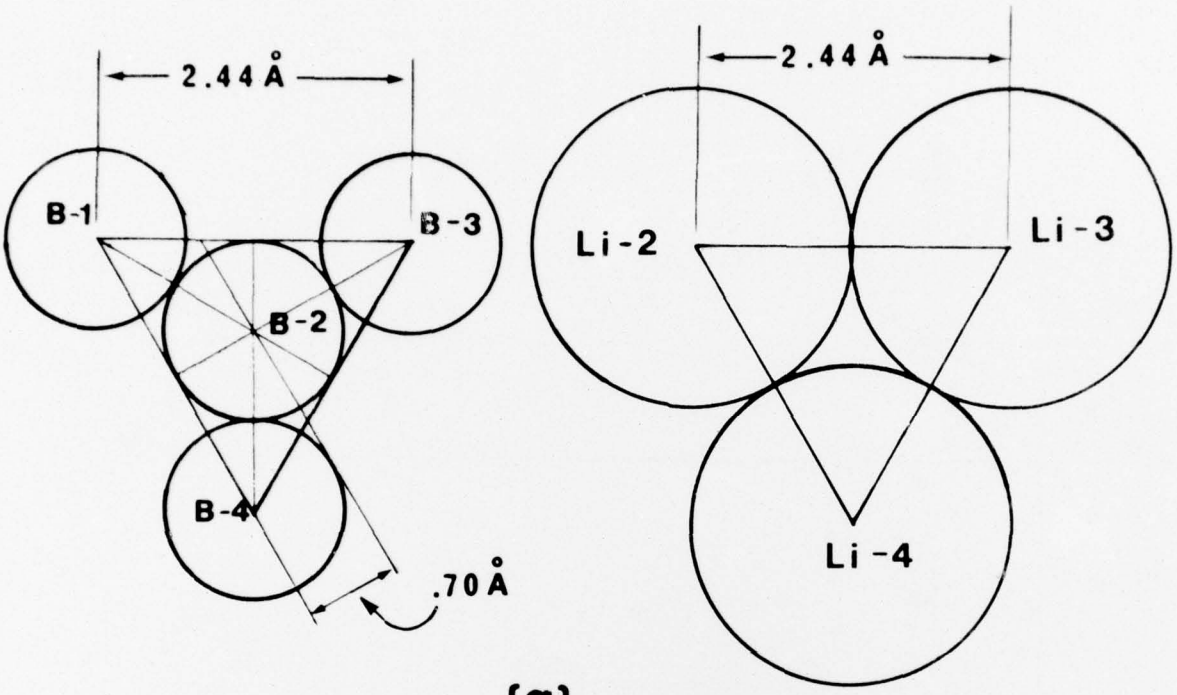

(a)

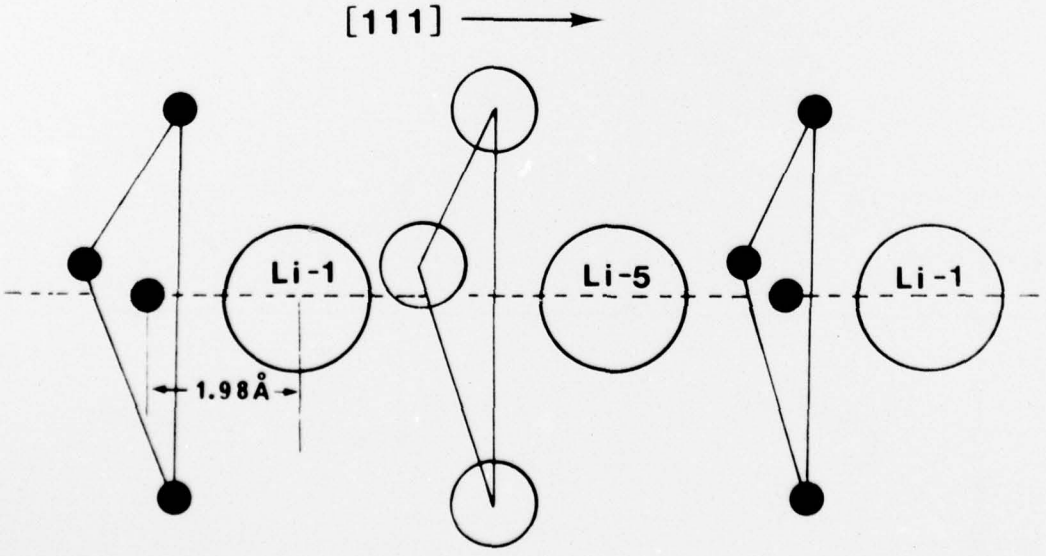

(b)

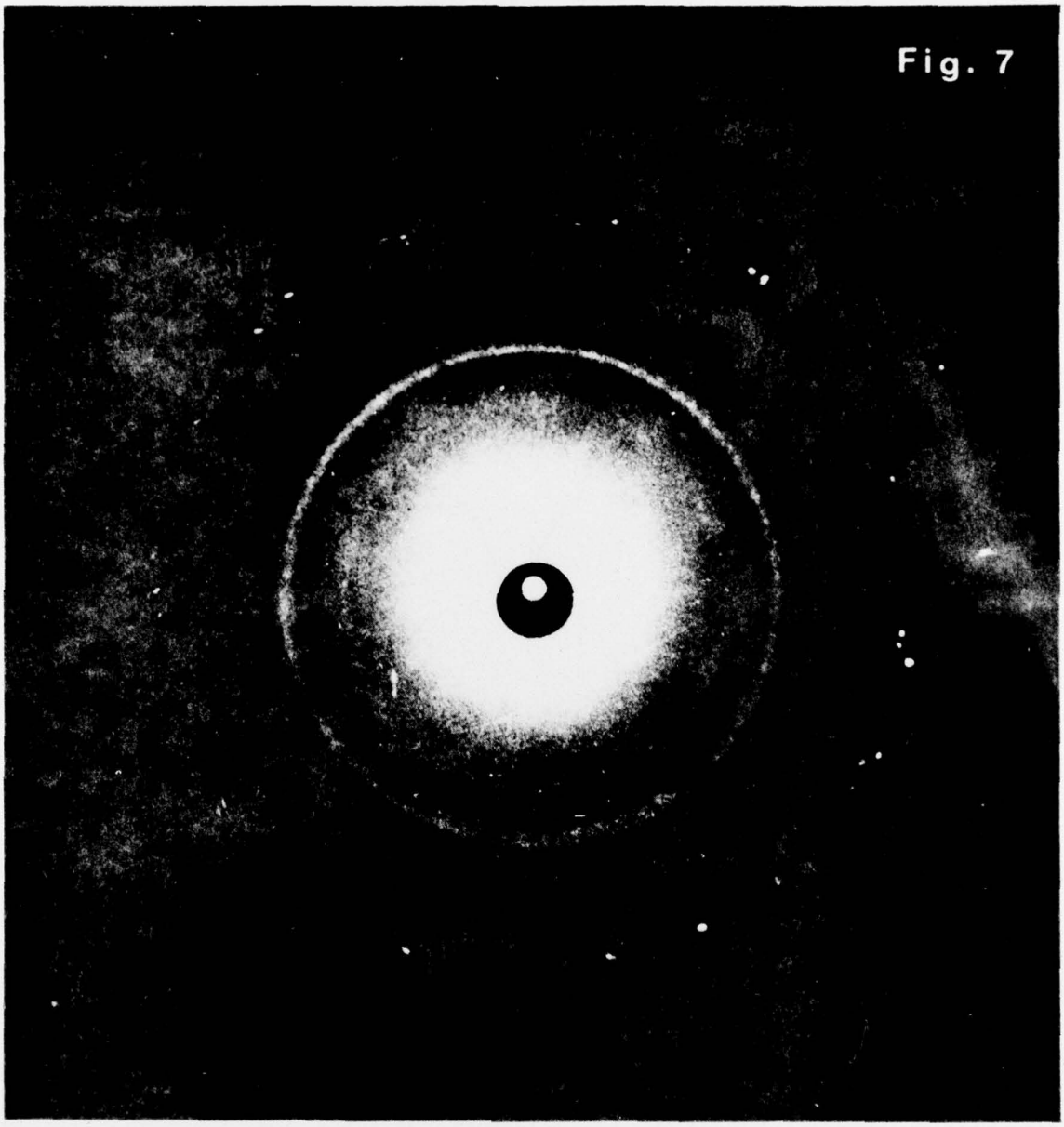
Fig. 7

Fig. 8

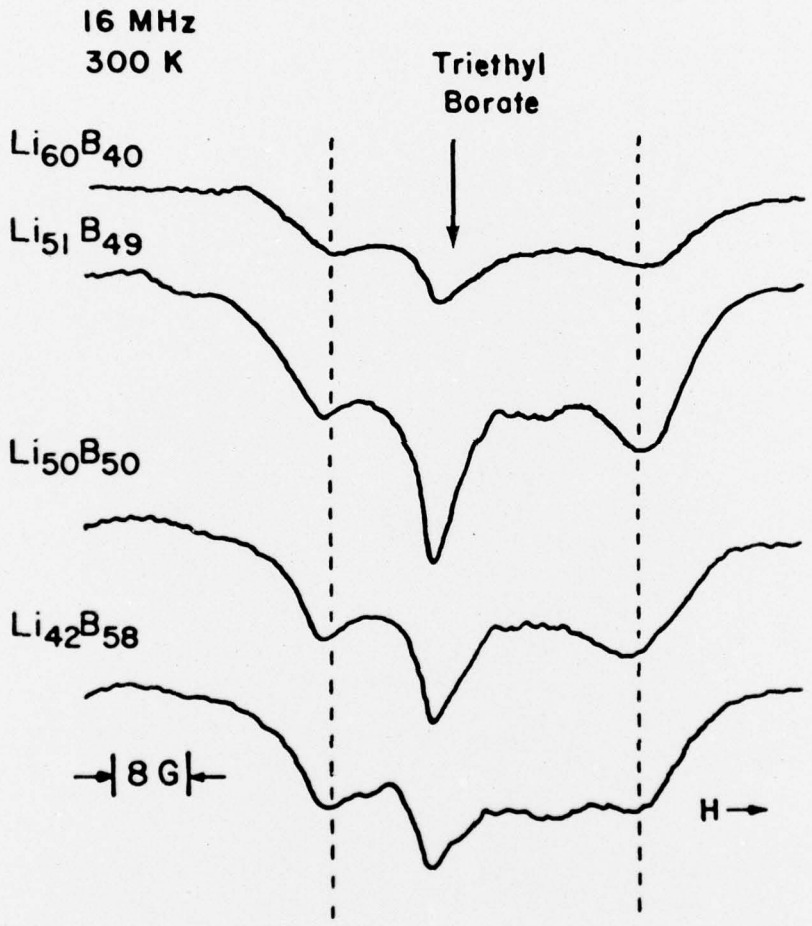
16 MHz
300 K
Triethyl
Borate
$Li_{60}B_{40}$
$Li_{51}B_{49}$
$Li_{50}B_{50}$
$Li_{42}B_{58}$
8 G
H

Fig. 9

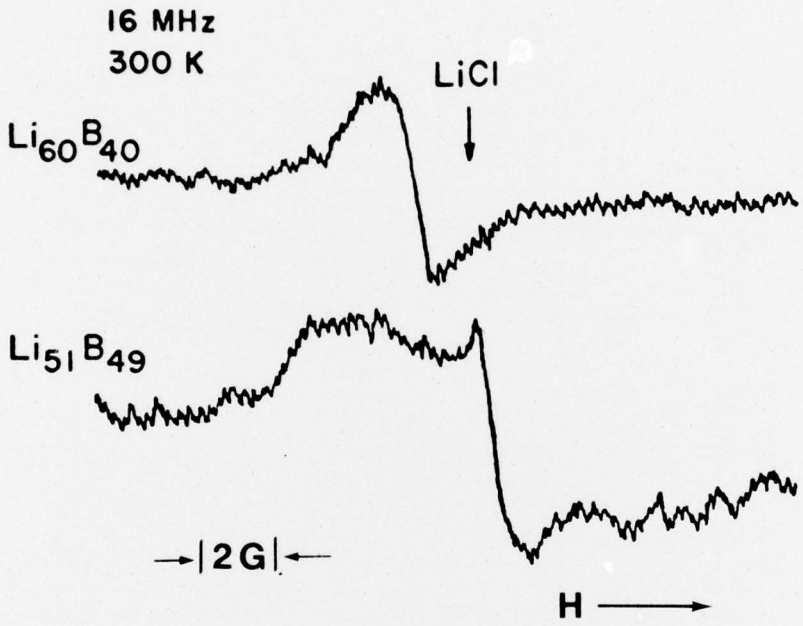

Fig. 10

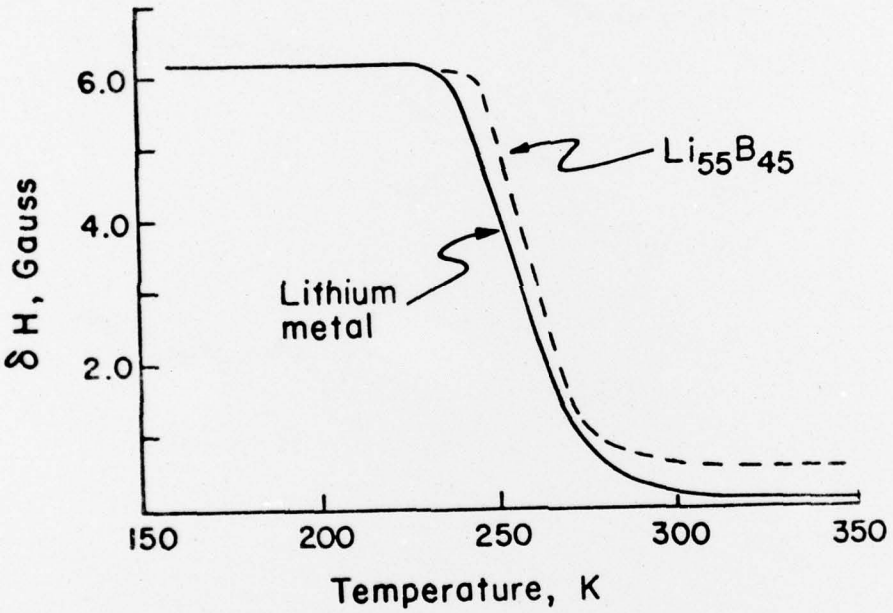
6.0
4.0
2.0
δ H, Gauss
Li55B45
Lithium
metal
150
200
250
300
350
Temperature, K

Fig. 11

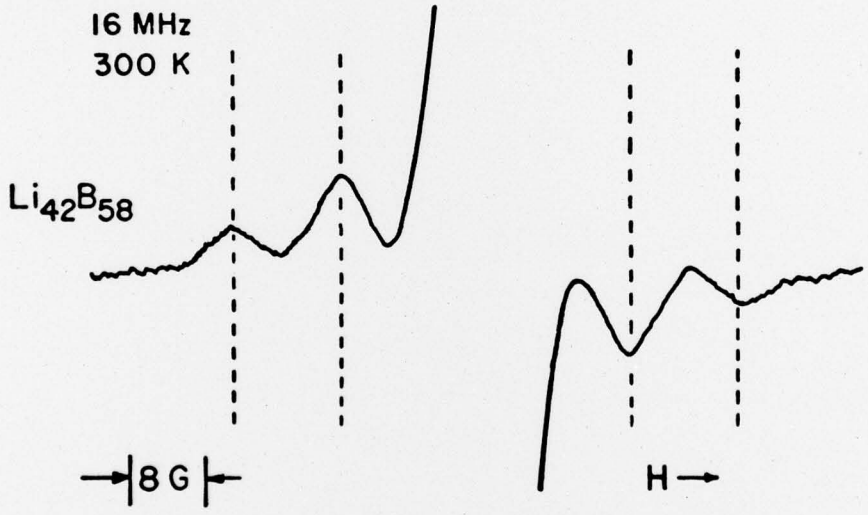

DISTRIBUTION LIST

Copies

Office of Naval Research
Department of the Navy
Washington, D. C. 20360
  Code 471
  Code 102
  Code 470

Commanding Officer
Office of Naval Research
Branch Office
495 Summer Street
Boston, Massachusetts 02210

Commanding Officer
Office of Naval Research
Branch Office
536 South Clark Street
Chicago, Illinois 60605

Office of Naval Research
San Francisco Area Office
760 Market Street, Room 447
San Francisco, California 94102
  Dr. P. A. Miller

Commander
Naval Research Laboratory
Washington, D. C. 20390
  Code 6000
  Code 6100
  Code 6300
  Code 6400
  Code 2627

Commanding Officer
Naval Air Development Center
Warminster, Pennsylvania 18974
  Code 302, Mr. F. S. Williams

Commanding Officer
Naval Air Propulsion Test Center
Trenton, New Jersey 08628
  Library

Commanding Officer
Naval Construction Batallion
Civil Engineering Laboratory
Port Hueneme, California 93043
  Materials Division

DISTRIBUTION LIST (Cont.)

Copies

Commanding Officer
Naval Ocean Systems Center
San Diego, California 92152
Electron Materials
Sciences Division
Library

Commanding Officer
Naval Missile Center
Materials Consultant
Code 3312-1
Point Mugu, California 93041

David W. Taylor Naval Ship R&D Center
Materials Department
Annapolis, Maryland 21402

Naval Underwater System Center
Newport, Rhode Island 02840
Library

Naval Postgraduate School
Monterey, California 93940
Mechanical Engineering Dept.

Commander
Naval Air Systems Command
Washington, D. C. 20360
Code 52031
Code 52032
Code 320

Commander
Naval Sea Systems Command
Washington, D. C. 20362
Code 035

Commanding Officer
Naval Facilities Engineering Command
Alexandria, Virginia 22331
Code 03

Scientific Advisor
Commandant of the Marine Corps
Washington, D. C. 20380
Code AX

DISTRIBUTION LIST (Cont.)

Copies

Naval Ship Engineering Center
CTR BG #2
3700 East-West Highway
Prince Georges Plaza
Hyattsville, Maryland 20782
Engineering Materials and
Services Office, Code 6101

Office of Chief of Research &
Development
Department of the Army
Energy Conversion Branch
Room 416, Highland Bldg.
Washington, D. C. 20315

Army Research Office
Box CM, Duke Station
Burham, North Carolina 27706
Metallurgy & Ceramics Div.

Army Materials and Mechanics
Research Center
Watertown, Massachusetts 02172
Res. Programs Office (AMXMR-P)

Air Force
Office of Scnentific Research
Bldg 410
Bolling Air Force Base
Washington, D. C. 20332
Chemical Science Directorate
Electronics and Solid State
Sciences Directorate

Air Force Materials Lab (LA)
Wright-Patterson AFB
Dayton, Ohio 45433

NASA Headquarters
Washington, D. C. 20546
Code RRM

National Aeronautics & Space
Administration
Goddard Space Flight Center
Greenbelt, Maryland 20771

NASA, Lewis Research Center
21000 Brookpark Road
Cleveland, Ohio 44135
Library

DISTRIBUTION LIST (Cont.)

Copies

National Bureau of Standards
Washington, D. C. 20234
  Metallurgy Division
  Inorganic Materials Division

Defense Metals and Ceramics
Information Center
Battelle Memorial Institute
505 King Avenue
Columbus, Ohio 43201

Director
Ordnance Research Laboratory
P. O. Box 30
State College, Pennsylvania 16801

Director, Applied Physics Laboratory
University of Washington,
1013 Northeast Fortheth Street
Seattle, Washington 98105

Metals and Ceramics Division
Oak Ridge National Laboratory
P. O. Box X
Oak Ridge Tennessee 37380

Los Alamos Scientific Laboratory
P. O. Box 1663
Los Alamos, New Mexico 87455
  Report Librarian
  Dr. C. Y. Huang, MS-704

Argonne National Laboratory
Metallurgy Division
P. O. Box 229
Lemont, Illinois 60439

Argonne National Laboratory
9700 South Cass Avenue
Argonne, Illinois 60439
  Mr. A. A. Chilenskas

Brookhaven National Laboratory
Technical Information Division
Upton, Long Island, New York 11973
  Research Library

Library
Building 50, Room 134
Lawrence Radiation Laboratory
Berkeley, California 94704

DISTRIBUTION LIST (Cont.)

Copies

Professor Y. N. Chiu
Department of Chemistry
Catholic University
Washington, D. C. 20017

Professor W. N. Lipscomb
Chemistry Department
Harvard University
Cambridge, Massachusetts 02138

Professor F. A. Kanda
Chemistry Department
Syracuse University
Syracuse, New York 13210

Professor C. W. Kern
Department of Chemistry
Ohio State University
140 West 18th Avenue
Columbus, Ohio 43210

Defense Documentation Center
Cameron Station
Alexandria, Virginia 22314 12